Sodium Photon Return, spot elongation and Fratricide effect: First on-sky results with GeMS

B. Neichel[1a], F. Rigaut[1], and M. Bec[2], M. Boccas[1], V. Fesquet[1], C. d'Orgeville[1], G. Trancho[2]

[1] Gemini Observatory - c/o AURA, Casilla 603 - La Serena, Chile
[2] GMTO Corporation - P.O. Box 90933 - Pasadena, CA 91109-0933

Abstract. GeMS, the Gemini MCAO system, is undergoing commissioning. Using 5 laser guide stars and a central launch, GeMS is particularly sensitive to Rayleigh backscatter and the fratricide effect. Using data covering a 5 months period from January to May 2011, we present results on (i) the Sodium return and its variability from night to night, (ii) the spot elongation and (iii) the fratricide effect. A simple modeling of the fratricide is presented as well as possible strategies for mitigation.

1 Introduction

The intrinsic properties and characteristics of the mesospheric sodium layer have come under intense investigation of late[1–3] due to the growing importance in producing sodium Laser Guide Stars (LGSs), and the increasing prevalence of such LGS systems on the world's leading telescopes. Sodium atoms are believed to be deposited in the high atmosphere by meteoritic ablation. They form a layer whose average altitude lies in the 90-95km altitude range above sea level, and can extend from 85 to 105km high. Significant abundance variations on hourly, daily and yearly time scales have been reported, even on time scales of a few minutes to a few hours. Typical seasonal variations are on the order of a factor of 2 to 4. The sodium layer mean altitude and width also exhibit significant variations on short and long time scales. Sodium abundance usually reaches its minimum in summer time and maximum in winter time, while the layer is in average lower in altitude (by 1 to 2km) and thinner (by 1km) at the equinoxes, and higher in altitude and thicker at the solstices. Most of the short time scale abundance and mean altitude variations can be traced down to the appearance of relatively short-lived, high density, thinner layers within the main sodium layer, which are subsequently called "sporadics"[4, 5].
It is the knowledge of the mesospheric sodium layer's short and long term behavior that will allow observatories to predict and maximize the performance of their respective LGS adaptive optics (AO) systems. This is particularly true for the future generation of Extremely Large Telescopes, as all of them are based on multi-LGS systems, and due to their large apertures they will be more sensitive to the Sodium variations.
GeMS is the Gemini MCAO system. It is the first multi-sodium based LGS AO system used for astronomy. It started on-sky commissioning in January 2011, at a rate of 5 to 7nights per month. This first period of commissioning last 5 months, after which GeMS entered a shutdown phase for engineering upgrades. During this first period of commissioning, we have gathered data about the sodium return, the spot elongation and the fratricide intensity. More details about GeMS and a description of the Laser can be found in companion papers[6–8].

2 Sodium Return

In fig.1-left we show the average sodium return measured for all the commissioning nights with good data. All the data has been taken at zenith, in the same conditions. Nights with clouds have been discarded. We do not use the data from January 2011 and February 2011, because at that time the

[a] bneichel@gemini.edu

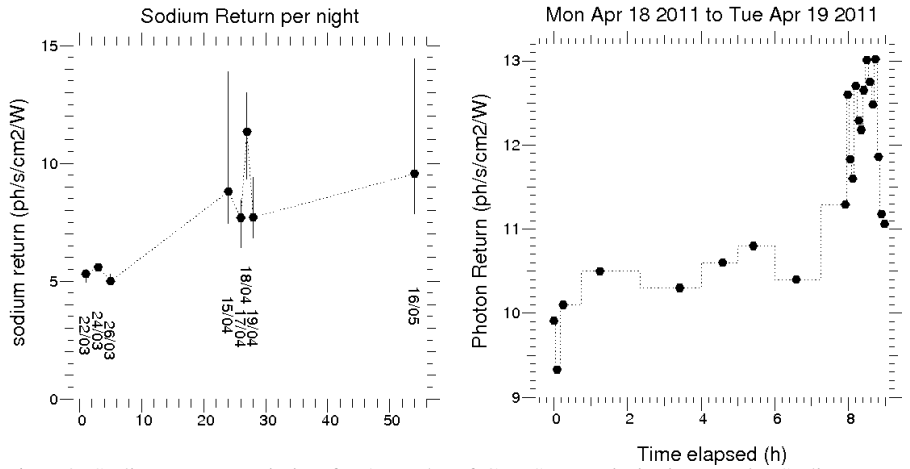

Fig. 1. *Left:* Sodium return variation for 3months of GeMS commissioning. *Right:* Sodium return variation for the night of the 18th to 19th April 2011.

laser spots were not yet optimized, and their Full-Width-Half-Maximum (FWHM) was bigger than the LGSWFS field stop, so flux measurements may be biased. From March on, laser spots were of the order of 1.3 to 1.5arcsec, which is smaller than the field of view of the LGSWFS subapertures of 2.8arcsec. For all these data points, the laser stabilization loop which is keeping each of the LGS in front of the LGSWFS was closed, so we do not expect flux loses because of coupling with the sub-aperture FoV.

We compute the flux in photons per seconds per cm^2 per Watt of laser propagated to the sky. The laser power at the output of the laser is monitored at a rate of 1Hz. The effective laser power projected into the sky has been calibrated with respect to the laser power, and the transmission of the Beam Transfer Optics has been measured to be 0.56. The photon return is measured at the LGSWFS level, so it includes all the loses due to transmission of the telescope itself, and Canopus (the AO bench). Our laser is circularly polarized, but the polarization was not optimized at the time of these measurements, so it may be more elliptical than purely circular. The wavelength of the laser was optimized for the best return, and locked during the nights. More details about the laser format can be found in a companion paper[8].

Fig. 1-left clearly shows the effect of the sodium season on the photon return: flux received in May is about twice time larger than what we measured in March. This is a known effect[2]: more return is expected in winter compare to summer, which unfortunatly is usually anti-correlated with the weather conditions and median seeing variation across the year. The second interesting feature to notice in Fig.1 is the amplitude of the variation within a night. The errors bars show the minimal and maximal return measured during each night: we see that we can experience variations by a factor of two to three. During this first commissioning period, we have empirically established that the high-order loop needs around 35ph/frame/pix to give good correction level. 35ph/frame/pix converts into 10 ph/s/cm2/W if we were running the loop at 800Hz. Results of Fig. 1-left shows that this conditions has only been achieved during 1 night in April, and part of a night in May. When we are in low sodium season, we have to lower the frame rate of the LGS loop, sometimes as low as 200Hz for the really "bad-sodium" nights. This is a limitation of the system, and may be improved in the future by improving the global throughput of the system and the laser power produced.

In Fig.1-right, we give more details of the variation of the sodium return within a given night. What's striking in this example, is that the flux suddenly increased by 50% at the end of night. This example may appear as exceptional, but we do observe sporadic like this every 2 or 3 nights (some statistics on sporadic events are presented in [3,9]).

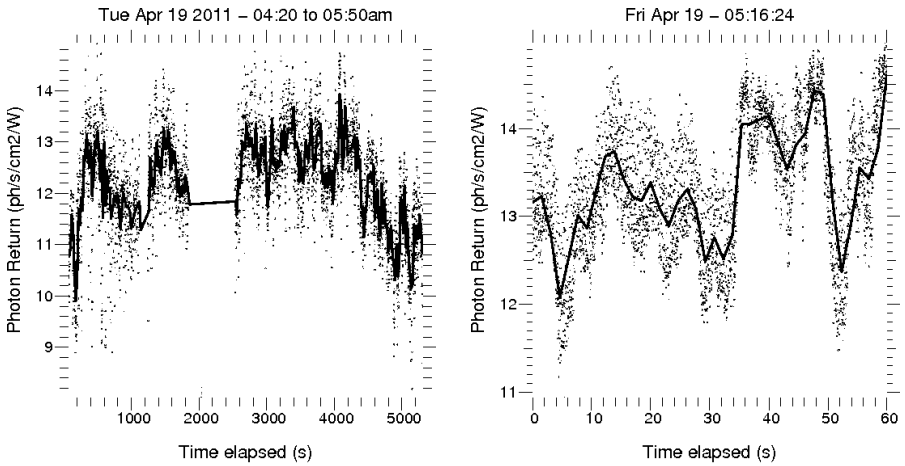

Fig. 2. *Left:* Sodium return over 2hours. *Right:* Sodium return over 1min.

In the plots of fig.2, we show the variation of the sodium return on shorter time scale. Plot on the left is covering 2hours at the end of the night of the 19th of April, and on the right, we zoom-in to illustrate variations over a timescale of 1 minute. Very fast variations could be due to laser power variations, as we monitor it only at 1Hz, but the global trend is supposedly only due to variation in the Sodium layer. All the plots of Fig.1 and 2 shows that the brightness of an LGS is nothing but constant, and that the amplitude of the variations can be significant. In order to take advantage of the sporadic, and also to limit the impact on performance when the flux decreases, we have implemented an automatic procedure that optimize the loop gains, frame rate and control matrix, based on the flux (and other atmospheric parameters, see[6]). We are also developing a database with all the flux measurements, that we eventually plan to use to optimize the scheduling of the laser operations. In the same way as we use the seeing or other atmospheric parameters, we plan to include the sodium return as a criteria in the observation queue planning. This information could also be used to calibrate theoretical models ([10, 11])

3 Spot elongation

Due to the vertical extension of the sodium layer, the WFS subapertures located far from the laser launcher see an elongated LGS image. In the small angle approximation, the angular elongation α is given by:

$$\alpha \simeq \frac{L.\Delta H}{H^2 + H\Delta H} \tag{1}$$

where ΔH is the thickness of the sodium layer, H is the low altitude of the sodium layer, and L is the distance between the pupil subaperture and the LGS launcher. For our case (8m telescope using central launch) the elongation is of the order of 1arcsec, and does not affect too much the measurements. This is however not the case anymore for the ELTs where the elongation can be as large as 10arcsec, and dramatically affect the ability to measure the wavefront[12]. As an illustrative example, we show in Fig.3 a picture of the LGS constellation that has been taken approximately 150 meter away from the launch telescope. With such an angle, laser spots appears to be ∼40arcsec, which is exactly the distance between two LGS spots following the diagonal of the constellation.

GeMS LGSWFS is using quad-cells, so we do not have a direct measurement of the spot size and elongation. To calibrate the spot size (which is an important parameter for the centroid gains) we use

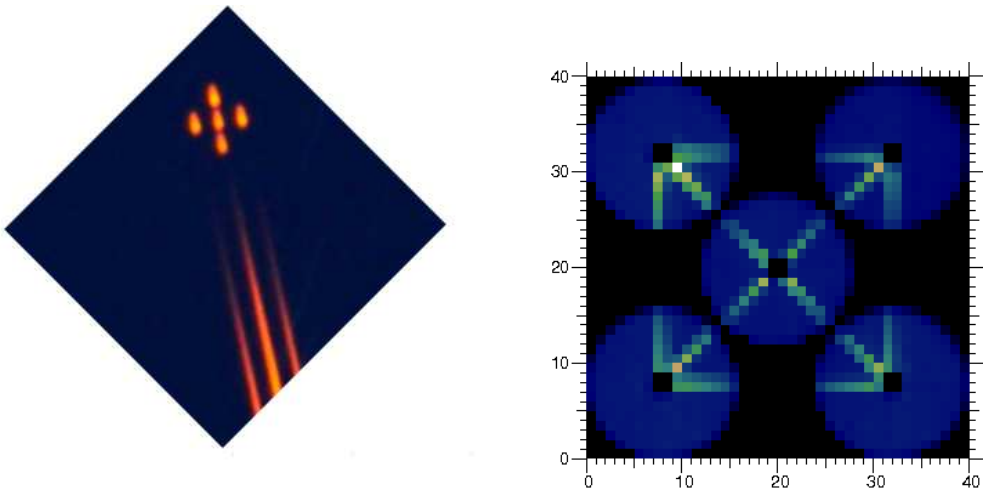

Fig. 3. *Left:* Close view of the LGS constellation. This picture has been taken ~150meter away from the telescope. *Right:* Image of the 5 LGSWFS that illustrates the impact of Fratricide.

a dithering method described in a previous paper[13]. This technique allows us to measure the spot size in X,Y and R, at a rate of 0.1Hz. Once one know the spot elongation (the R parameter), and assuming a constant altitude of 90km for the sodium layer, we can invert Eq.1 and derive the sodium layer thickness.
During the first commissioning period, very few data has been recorded regarding spot elongation. In fig.4-left we show the data for the night of the 17th of April. Plot on the left shows the evolution of the centroid gains (parameter which is directly proportional to the size of the spot) with the seeing. When seeing gets worst, we expect to have bigger LGS spots, which explains the correlation seen in fig.4-left. In fig4-right, we plot the derived sodium layer thickness evolution with time, for the same data points. We do see variations of the order of few kilometers, which is in good agreement with higher resolution measurements[1]. Note however that the results presented below are still preliminary, and we are consolidating our database with better measurement points.

4 Fratricide effect

The so-called fratricide effect is due to the scattering of laser photons on dust or cloud particles (Mie scattering on aerosols and cirrus) or on air molecules (Rayleigh scattering) located along a laser beam projected to the sky. In multi-LGS systems, a fraction of the back-scattered light from each of the laser beams ends up being collected by WFSs observing the other LGSs. The fratricide effect is prominent mostly for systems that launch all the laser beams from near the center of the primary mirror (e.g., behind the secondary mirror). The effect is also stronger at higher zenith angles. A detailed description of the fratricide effect can be found in [14, 15] and a 3D animation of the fratricide is available on the AO4ELT website[1].
The fratricide effect creates a strong background on specific subapertures, which could biases the slopes measurements. In fig.3-right, we show an example of the subapertures illumination. The specific "X-shape" form of the fratricide is due to the constellation geometry.
In order to simulate the fratricide effect, we have developed a simple model that reproduces the flux intensity. As a first-order approximation, it can be assumed that the laser beams at low altitude where

[1] http://ao4elt2.lesia.obspm.fr/spip.php?article563

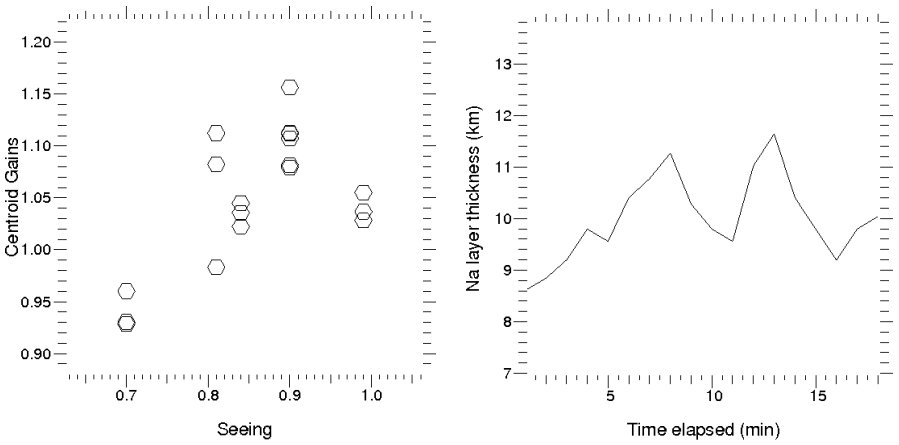

Fig. 4. *Left:* Centroid gains (or LGS spot size) variations with seeing. *Right:* Sodium layer thickness evolution with time.

scattering occurs are completely out of focus for the WFS. For this reason the photon return flux from Rayleigh backscattering can be considered as an homogeneous background received by a single subaperture. Then each laser beam is sampled in altitude with an arbitrary resolution of few km. The contribution of each slab of laser beam on the WFS is then simply modeled as a Gaussian with the proper position angle with respect to the subaperture. For instance, in fig5-left, we show how the beams would be seen by each WFS for a slab located 17.2km above the telescope. The FWHM of the Gaussian is set by a quadratic sum of the laser beam diameter, the seeing, and the blur caused by the beam defocus. We simply assume that the intensity of the laser is exponentially decreasing with the altitude, with a typical scale height of 5km. Note that we do not introduce any r^{-2} dependence to account for a perspective effect, as we believe this is canceled-out by a similar (but opposite in sign) perspective effect due to the subaperture FoV. This assumption is only valid when the laser beam completely covers the subaperture FoV, which is true for our case.

We use this simple model to fit (with a Levemberg-Marquart method) the real data. Figure 6 shows a typical result of these fits. Free parameters include scale height, total and relative flux for each beam, LGS constellation position in the sky (offset and rotation), position of each beam on the LLT, FWHM of the Gaussian beams (constant for all the altitudes).

Residual of the fits are of the order of few counts, which demonstrates that our analytical form is correct. Note that the offset of the constellation, rotation and position of beams on the LLT are used to aligned the constellation (see [7]). It also interesting to note that typical scale height that we found are of the order of 5km, which is in good agreement with the average scale height of earth, as reported by the US Naval Research Laboratory[2]. They report an average scale height of 7.64km, which is close to the 5km found above, to which we add the altitude of Cerro Pachon which is 2.6km

As we introduced earlier, the fratricide creates a strong background on specific subapertures. Depending on the sodium season and the amount of dust contains in the atmosphere, the ratio Rayleigh / Sodium will change. Subaperture closer to the center of the pupil are also more affected than the outside ones. Typical numbers that we measured show that this ratio is ranging from 30 to 10 for the subaperture close the center of the pupil, and down to ∼1 to 3 for subapertures at the border of the pupil. This background is attenuating the slopes and strongly biasing the quad-cell signal. The question is then: “can we calibrate properly this background, and get rid of the fratricide”. It is an important

[2] www.nrl.navy.mil/research/nrl-review/2003/atmospheric-science/picone/

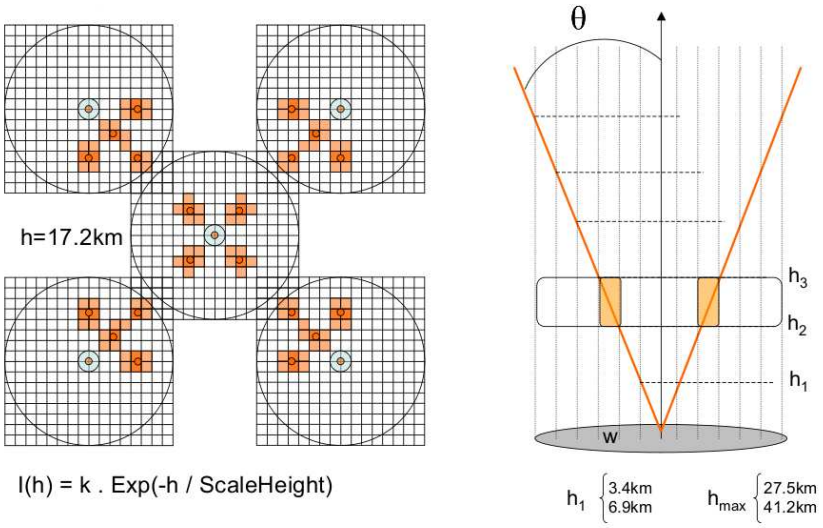

Fig. 5. Modeling of the fratricide effect.

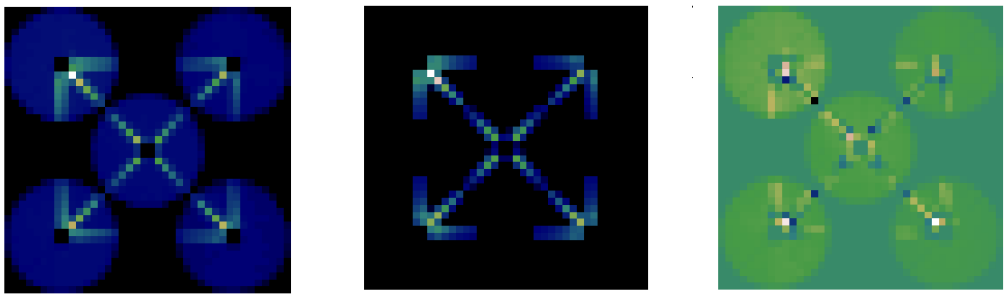

Fig. 6. *Left:* LGSWFS data. *Middle:* Fit to the data. *Right:* Residual (Data - Fit).

question that also drives the choice for the future generation's AO systems, and which has been as the center of previous studies [16, 17, 12, 14].

The baseline strategy that was foreseen for GeMS was the following: (1) Detune the laser out of the 589nm band; (2) Acquire a dark with the LGSWFS; (3) subtract the dark. This was supposed to be done regularly during the night, every few hours or so. Unfortunately, we found that this method was deficient, because the Rayleigh background was not constant. The main reason for the variation of the Rayleigh background is due to the LGS stabilization loop. This loop uses 5 Tip-Tilt platforms to drive the LGS in-front of the LGSWFS. This loop can run up to 400Hz, and allows to compensate for the up-link Tip-Tilt. But the Tip-Tilt platforms are not located in a pupil plane, and when the LGSs move on the far-field (on the sky) the beams also move on the near-field (on the LLT). According to the optical drawings, we estimate the jitter of the beams on the LLT to be of the order of 10mm rms. Depending on the location of the beams on the LLT, the fratricide will affect different subapertures. As a matter of fact, if we subtract a dark for a given position of the beams on the LLT, this will not be valid anymore as soon as this stabilization loop is closed. For some of the frames, the subtraction will

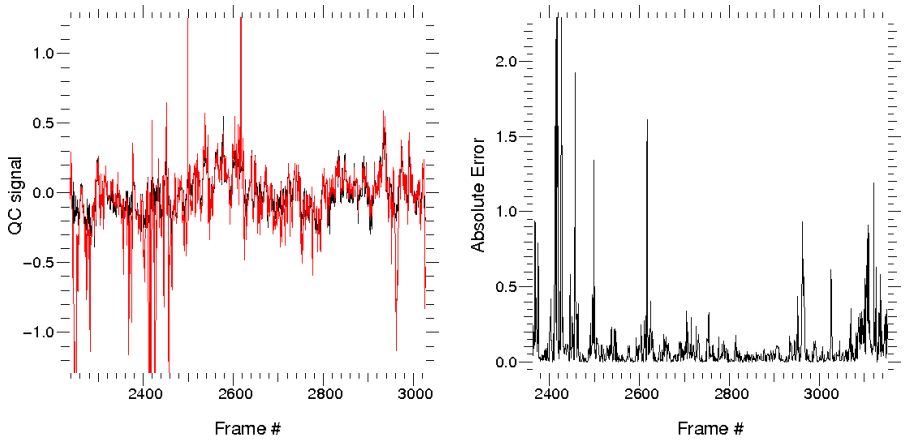

Fig. 7. *Left:* Centroid gains (or LGS spot size) variations with seeing. *Right:* Sodium layer thickness evolution with time.

be good, but for other we will over or under subtract the Rayleigh background for some subapertures. In the plots of fig.7, we show what would be the impact of this wrong subtraction on the slopes. For this, we have computed the quad-cell signal for a sample subaperture not affected by the Rayleigh background (in black in the plot fig.7-left). Then, we add to this subaperture the residual intensity variations due the wrong Rayleigh subtraction, and we re-compute the quad-cell signal (in red in the plot fig.7-left). The absolute difference between these two cases is shown on the plot of fig.7-right. As predicted, we see that for some frames the background subtraction is good, and we could use the signal coming from these slopes, but for some other frames, the error is significant. To fully address the impact of this effect, we would need to propagate this error in the tomographic reconstructor, and evaluate what is the impact on the reconstructed phase.

So far, and given that we cannot properly calibrate the Rayleigh background, the strategy that we have followed is to discard all the subapertures that are affected by the fratricide on the reconstruction process. This represents 224 subapertures or 22% of all the subapertures. The effect is that some actuators on the DMs are now less seen, or even completely not seen at all as it is the case for the 4 central actuators of DM4.5. In fig.8 we show the rms of the interaction matrix in an actuator basis. The color coding would be equivalent to the sensitivity of each actuator, or in other words: “how well an actuator is seen by the WFS”. Top line shows the maps for DM0, DM4.5 and DM9 respectively, when all the subapertures are used. Bottom line shows the same maps, when we discard all the subapertures affected by the Rayleigh background. We see that the sensitivity of the system is lower, but because we have enough spatial redundancies, we can still operate.

5 Conclusions

GeMS is the first multi-LGS system in operation for astronomy. First results obtained on-sky are then very instructive, as they show what works and what are the limitations. Our main conclusions about the LGS are:

- With our laser format, and given the throughput of the Beam Transfer Optics, 50W of laser power is short during the low sodium season.
- The brightness of the LGS can change rapidly, and by large factors. Systems should take advantage of the sporadic, and try to reduce the impact of low return.
- Calibrating the Rayleigh background is challenging (but not impossible), and dedicated real-time (or close to real-time) procedures should be developed to do it properly.

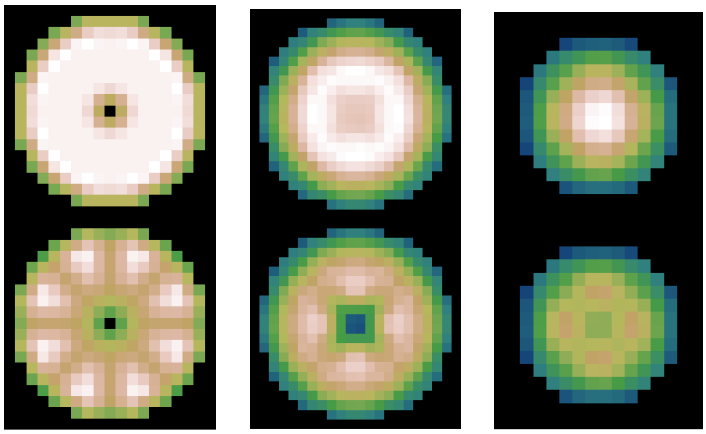

Fig. 8. Top: Bottom: . From left to right: DM0, DM4.5, DM9.

– The design of the Beam Transfer Optics is crucial as it also impacts the Rayleigh background.
– Rayleigh background is very sensitive to the presence of clouds, and thin cirrus, and Rayleigh intensity can change rapidly.

The Gemini Observatory is operated by the Association of Universities for Research in Astronomy, Inc., under a cooperative agreement with the NSF on behalf of the Gemini partnership: the National Science Foundation (United States), the Particle Physics and Astronomy Research Council (United Kingdom), the National Research Council (Canada), CONICYT (Chile), the Australian Research Council (Australia), CNPq (Brazil), and CONICET (Argentina).

References

1. T. Pfrommer, P. Hickson, and Chiao-Yao She, 1st AO4ELT conference, **04001**, 2010
2. N. Moussaoui, B. R. Clemesha, R. HolzlÃ¶hner, et al., A&A **511**, 2010, A31
3. T. Pfrommer, and P. Hickson, JOSA-A, **27**, 2010, 11
4. B. R. Clemesha, H. Takahashi, Advances in Space Research, **16**, 1995, 141-149
5. B. R. Clemesha, P. P. Batista, and D. M. Simonich, Journal of Geophysical Research, **101-A9**, 1996, 701-706
6. B. Neichel, F. Rigaut, M. Bec, M. Boccas, SPIE, **7736**, 2010, 773606
7. F. Rigaut et al., This conference, 2012
8. C. d'Orgeville et al., This conference, 2012
9. C. d'Orgeville, F. Rigaut, M. Boccas, C. Dainty et al., SPIE, **4839**, 2003, 492-503
10. R. Holzlohner, S.M. Rochester, D. Bonaccini Calia, D. Budker, A&A, **510** 2010, 20H
11. N. Moussaoui, R. Holzlohner, W. Hackenberg, and D. Bonaccini Calia, A&A **501**, 2009, 793-799
12. C. Robert, J.-M. Conan, D. Gratadour, JOSA-A, **27**, 2010, 11
13. D. Gratadour, F. Rigaut, OSA Topical Meetings, **PMA4**, 2007
14. L. Wang, A. Otarola, and B. Ellerbroek, JOSA-A, **27**, 2010, 11
15. D. Gratadour, E. Gendron, G. Rousset and F. Rigaut, 1st AO4ELT conference, **04005**, 2010
16. M. Tallon, I. Tallon-Bosc, C. Bechet and E. Thiebaut, SPIE, **7015**, 2008, 70151N
17. L. Gilles, L. Wang, and B. L. Ellerbroek, Apl. Opt, **49**, 2010, 31